

## Propagation of an asymmetric relativistic laser pulse in plasma

D. P. Garuchava, I. G. Murusidze, G. I. Suramlishvili, N. L. Tsintsadze, and D. D. Tskhakaya  
*Institute of Physics, Georgian Academy of Sciences, 380077 Tbilisi, Georgia*  
 (Received 6 May 1996; revised manuscript received 3 June 1997)

The interaction of a relativistically intense asymmetric laser pulse with a plasma has been studied. The asymmetric shape of the pulse implies that the rise time of the leading edge of the pulse is much greater than the fall time of the trailing edge. The numerical simulation of the propagation of such a pulse through an underdense plasma has shown that relativistic self-focusing enhances the effect of ponderomotive self-channeling. The radial ponderomotive force totally expels the electrons from the axis creating a density channel, that is, cavitation occurs. A very short fall time of the trailing edge ( $\tau_l \omega_p \ll 1$ ) causes a rapid increase in the amplitude of a laser driven longitudinal electric field to values of a few GV/cm at the back of the pulse. The numerical simulation also has shown that the channel as well as the large-amplitude longitudinal field can be sustained in the range immediately behind the pulse, thus creating favorable conditions to accelerate a trailing bunch of electrons to extremely high energies. According to our model, the accelerating electric field can reach the value 10 GV/cm. [S1063-651X(97)04609-6]

PACS number(s): 52.40.Nk, 42.65.Jx, 52.35.Mw, 52.40.Db

The interaction of a relativistically intense laser pulse with plasmas and accompanying phenomena are of great interest because of their importance to plasma-based accelerators in which the plasma wave is driven by a single ultrahigh-intensity laser pulse. This scheme, referred to as the laser wake-field accelerator, has been developed as one of the promising plasma-based accelerators [1].

Ultrashort laser pulses ( $\omega_p t_L \lesssim 1$ , where  $\omega_p$  is the electron plasma frequency and  $t_L$  is the pulse duration) undergo Rayleigh diffraction, which significantly decreases the pulse intensity over a few Rayleigh lengths. This limits the laser-plasma interaction distance and makes the generation of plasma wake fields inefficient. For relatively long pulses ( $\omega_p t_L \gg 1$ ), relativistic self-focusing as well as ponderomotive self-channeling can efficiently prevent the diffraction. Both mechanisms of self-guiding were taken into account in [2] studying the propagation of a circularly polarized radiation through plasmas. It is noted that, for certain laser-plasma parameters, plasma electrons will be completely expelled from the focal area. The detailed study of the phenomenon has shown that, beginning from certain pulse intensities, a sufficiently long ion channel forms along the pulse propagation direction [3].

As a rule, only a slight portion of the energy of a laser pulse is transferred to generated longitudinal fields. If the duration of the pulse is much longer than the period of electron plasma oscillations, then the ion channel behind the pulse disappears and the wake field following the pulse will not be effective for acceleration [3]. To avoid these difficulties a concept of an asymmetric laser pulse has been proposed [4]. As shown below, a pulse with asymmetric longitudinal and radial profiles has advantages over a symmetric one. An asymmetric pulse creates an ion channel that ensures its diffractionless propagation over many Rayleigh lengths. At the same time, a laser-driven plasma wake field reaches high values at the back of the pulse. Moreover, this field, along with the ion channel, can be sustained over the short fall length of the trailing edge of the pulse. All these are favorable conditions for acceleration.

Considering an asymmetric pulse, we assume that the duration of the leading edge of the pulse  $\tau_l$  is much greater than the period of the electron plasma waves  $(\omega_p \tau_l)^2 \gg 1$ , while the opposite inequality holds at the trailing edge,  $(\omega_p \tau_r)^2 \ll 1$ ,  $\tau_r$  being the time scale of the back of the pulse (see Fig. 1). These conditions ensure a relatively smooth rise of a laser-driven longitudinal electric field at the front. This field does not exhibit the oscillating nature within the leading edge of the pulse, in accordance with the results obtained in [5]. At the same time, unlike the previous works quoted here, the transverse scales of the pulse profile  $l_{\perp l}, l_{\perp r}$ , which correspond to the front and the back of the pulse, respectively, satisfy the conditions

$$(\lambda_0)^2 \ll l_{\perp l}^2 \ll (c \tau_l)^2, \quad (\lambda_0)^2 \ll (c \tau_r)^2 \ll l_{\perp r}^2, \quad (1)$$

where  $\lambda_0 = 2\pi c \omega_0^{-1}$  is the laser wavelength. The period of the laser wave is much less than the duration of both the leading and trailing edges  $(\omega_0 \tau_l)^2 \gg 1$  and  $(\omega_0 \tau_r)^2 \gg 1$ . Consequently, on both of the edges one can distinguish two time scales. In accordance with this, any of the quantities  $S = (\vec{P}, n, \vec{E}, \Phi, \gamma)$  appearing in the problem are represented as a sum of slowly and fast varying terms

$$S = \langle S \rangle + \tilde{S}, \quad (2)$$

where the symbol  $\langle \rangle$  denotes a time average over the laser wave period  $\sim 2\pi/\omega_0$ ,  $\vec{P}$  is the momentum of the electrons,

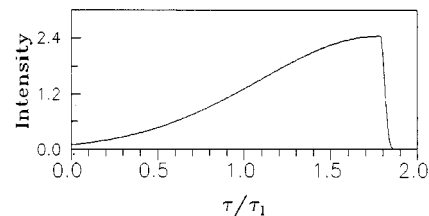


FIG. 1. Profile of the normalized intensity  $I = (e|E|/mc\omega_0)^2$  of an asymmetric pulse with Gaussian rise and fall,  $(\tau_l/\tau_r)^2 = 10^3$ .

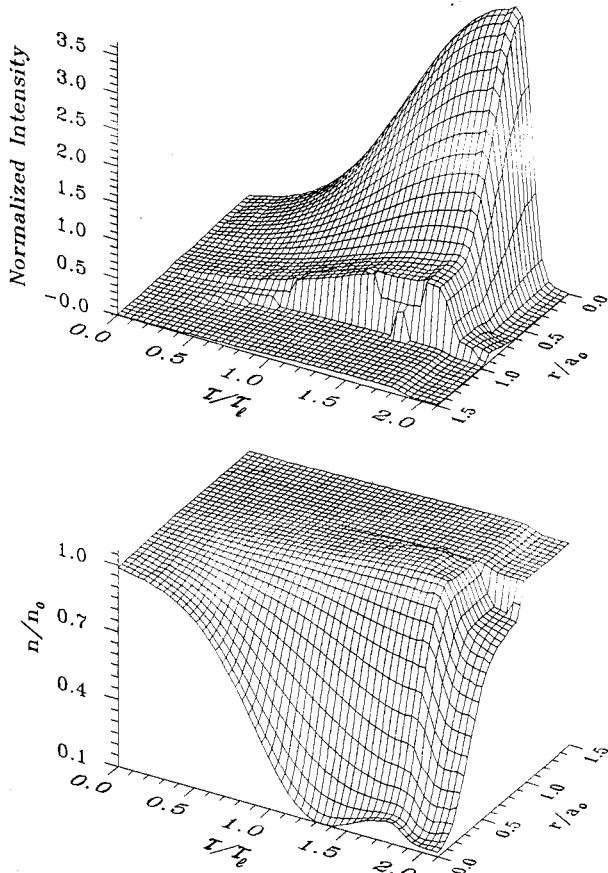


FIG. 2. Normalized intensity distribution of a laser pulse and the corresponding profile of the plasma electron density after traveling the distance  $0.4L_R$  [ $L_R = \pi(a_0^2/\lambda_0)$  is the Rayleigh length]. It shows one of the first stages of the ion-channel formation.

$n$  is their density,  $\vec{E}$  is the electric field,  $\Phi$  is the potential of the generated longitudinal field, and  $\gamma$  is the relativistic factor. Characteristic velocities in our problem are much larger than the thermal velocities of electrons, thus the hydrodynamic description seems to be quite justified. The corresponding set of equations consists of the equation of motion for electrons (ions are immobile) and Maxwell's equations. Let us introduce the dimensionless quantities  $\vec{P}/mc \rightarrow \vec{P}$ ,  $e\Phi/mc^2 \rightarrow \Phi$ ,  $n/n_0 \rightarrow n$ , and  $e\vec{E}/mc\omega_0 \rightarrow \vec{E}$ . In this case for slowly varying quantities we obtain the equations

$$\frac{1}{c^2} \frac{\partial^2 \langle P \rangle}{\partial t^2} - \Delta \langle \vec{P}^l \rangle + \frac{1}{c} \frac{\partial}{\partial t} \vec{\nabla} \langle \gamma \rangle + \frac{\omega_p^2}{c^2} \langle \vec{J} \rangle = 0, \quad (3)$$

$$\frac{1}{c} \frac{\partial \langle n \rangle}{\partial t} + \text{div} \langle \vec{J} \rangle = 0, \quad (4)$$

$$\frac{1}{c} \frac{\partial \langle \vec{P}^l \rangle}{\partial t} = \vec{\nabla} \langle \Phi \rangle - \vec{\nabla} \langle \gamma \rangle, \quad (5)$$

$$(c^2/\omega_p^2) \nabla \langle \Phi \rangle = \langle n \rangle - 1, \quad (6)$$

where the superscripts  $l$  and  $t$  denote the longitudinal and transverse components of a vector, respectively. The fast

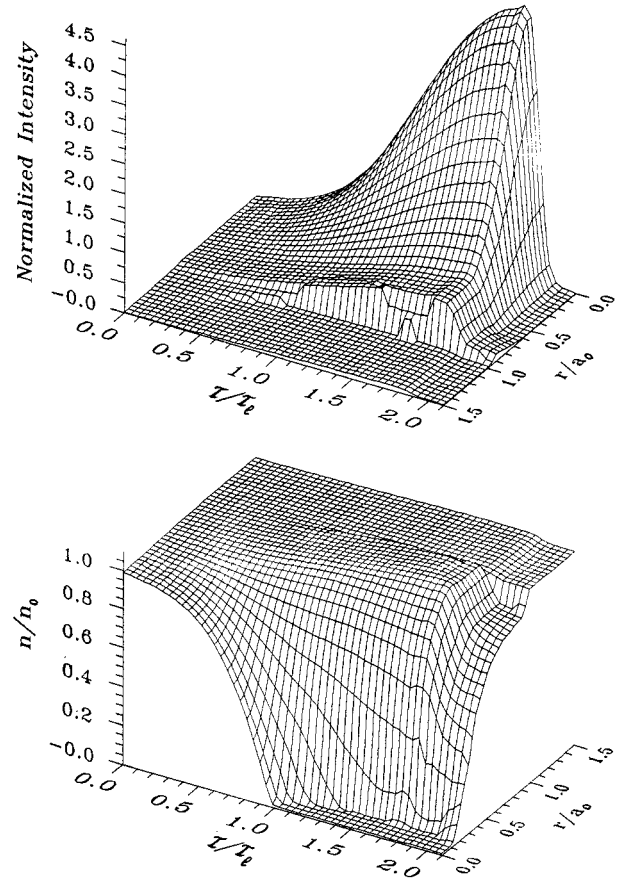


FIG. 3. Intensity and electron density profiles after the pulse has traveled the distance  $0.5L_R$ . The ion channel is formed and continues to evolve, which is seen in subsequent figures.

transverse momentum is represented in the form  $\vec{P}_\perp^t = \frac{1}{2}(\vec{e}_r + i\vec{e}_\varphi)P(r, z, t)\exp\{-i\omega_0 t + ik_0 z + i\varphi\} + \text{c.c.}$ , where  $\vec{e}_r, \vec{e}_\varphi$  are the unit vectors along the radial and azimuthal axes, respectively,  $\varphi$  is the azimuthal angle, and  $\omega_0 = k_0 c$ . The equations for fast varying quantities are obtained from Eqs. (3)–(6) by substituting  $\langle S \rangle \rightarrow \tilde{S}$ . However, it should be noted that for the relativistic factor we have

$$\langle \gamma \rangle = \{1 + \tilde{P}^2 + \langle \vec{P} \rangle^2\}^{1/2}, \quad (7)$$

$$\tilde{\gamma} = (\tilde{P}/\langle \vec{P} \rangle) \langle \gamma \rangle \ll \langle \gamma \rangle. \quad (8)$$

Expressions for  $\langle \vec{J} \rangle$  and  $\tilde{\vec{J}}$  are rather cumbersome. They can be easily obtained and therefore we do not write them down. We only mention that by using  $\text{rot} \vec{P}^l = 0$  and  $\text{div} \vec{P}^t = 0$  some relations are established between momentum components that can help to obtain the following formulas for the slow and fast currents, respectively:  $\langle \vec{J} \rangle = \langle n \rangle \langle \vec{P} \rangle / \langle \gamma \rangle$  and  $\tilde{\vec{J}} = \langle n \rangle \tilde{\vec{P}} / \langle \gamma \rangle$ .

We introduce the variables  $\xi = z$  and  $\tau = t - z/c$ . Taking into account the profile of the pulse front, which is characterized by inequalities (1), for the leading edge of the pulse, Eqs. (3)–(6) are reduced to the system [3]

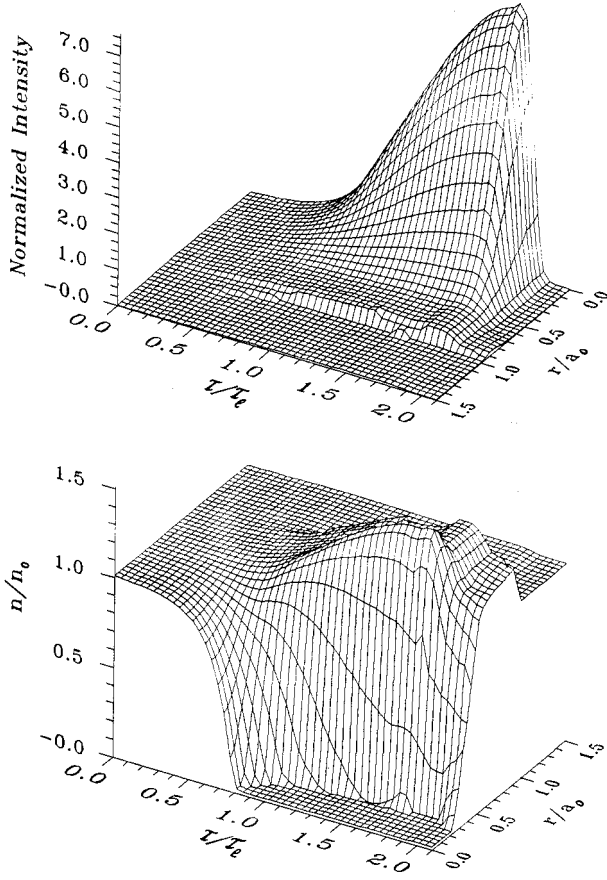


FIG. 4. Intensity and electron density profiles after propagating the distance  $L_R$ . The width and length of the channel are increased compared to Fig. 3.

$$2ik_0 \frac{\partial E}{\partial \xi} + \Delta_{\perp} E - \frac{\omega_p^2 \langle n \rangle}{c^2 \langle \gamma \rangle} E = 0, \quad (9)$$

$$\frac{1}{r} \frac{\partial}{\partial r} r \frac{\partial \langle \Phi \rangle}{\partial r} = \frac{\omega_p^2}{c^2} (\langle n \rangle - 1), \quad (10)$$

$$\langle n \rangle = 1 + \frac{c^2}{\omega_p^2} \frac{1}{r} \frac{\partial}{\partial r} r \frac{\partial \langle \gamma \rangle}{\partial r} \geq 0, \quad (11)$$

$$\langle \gamma \rangle = \{1 + |E|^2\}^{1/2}, \quad (12)$$

where  $E = -iP$  is the amplitude of the laser field. The following boundary and initial conditions are added to these equations:

$$\begin{aligned} |E|^2(r, \xi=0, \tau) &= |E_0|^2 \exp\{-r^2/a_0^2 - \tau^2/\tau_1^2\}, \\ n(r, \xi, \tau = -\infty) &= 1, \end{aligned} \quad (13)$$

$$\Phi(r, \xi, \tau = -\infty) = 0, \quad \partial |E(r=0, \xi, \tau)| / \partial r = 0.$$

At the back of the pulse, the averaged quantities  $\langle S \rangle$  vary slowly in the radial direction on the scale of the back of the pulse  $c\tau$ . This implies that

$$\partial \langle S \rangle / \partial r \ll c^{-1} \partial \langle S \rangle / \partial \tau. \quad (14)$$

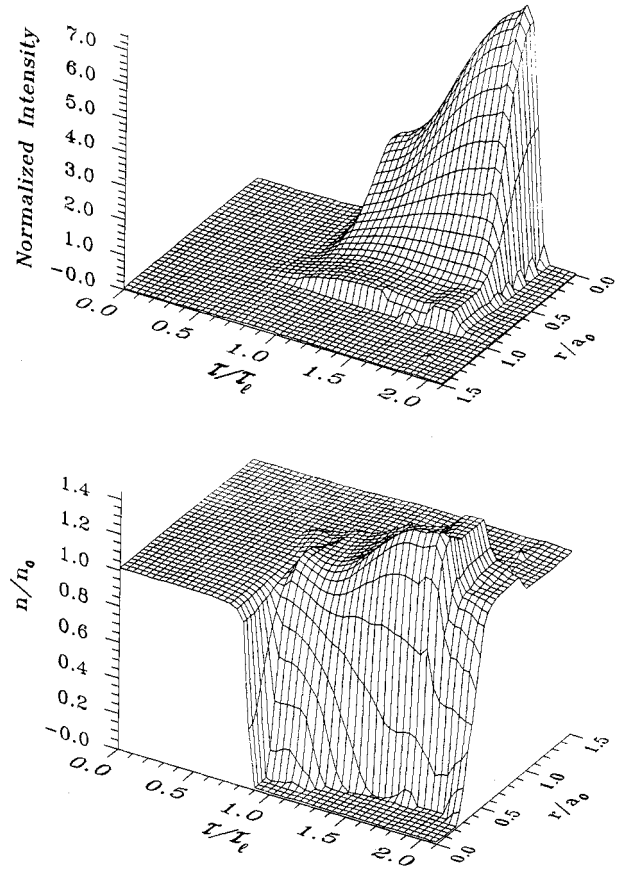


FIG. 5. Intensity and electron density profiles after the pulse has traveled the distance  $8L_R$ . A strong redistribution of the pulse intensity and the electron density at the leading front of the pulse is evident.

In addition, we have

$$\partial \langle S \rangle / \partial z \approx -c^{-1} \partial \langle S \rangle / \partial \tau. \quad (15)$$

By using Eqs. (14) and (15) with the help of equations  $\text{rot} \langle \vec{P}^l \rangle = 0$  and  $\text{div} \langle \vec{P}^l \rangle = 0$  one can establish the relations

$$\langle P_r^l \rangle \approx \langle P_r^l \rangle \ll \langle \gamma \rangle, \quad \langle P_z^l \rangle \ll \langle P_r^l \rangle. \quad (16)$$

At the same time, as shown below,  $\langle P_r^l \rangle$  does not change appreciably at the trailing edge

$$\langle P_r^l \rangle \approx \langle P_r^l \rangle_0, \quad (17)$$

where  $\langle P_r^l \rangle_0$  is the value of  $\langle P_r^l \rangle$  at the end of the front. The equation for the laser field amplitude at the back of the pulse contains a mixed derivative. This will enable us to describe the variation of the trailing edge of the pulse. Under condition (14), this equation has the form

$$2ik_0 \frac{\partial E}{\partial \xi} - 2 \frac{\partial^2 E}{\partial \xi \partial \tau} - \frac{\omega_p^2 \langle n \rangle}{c^2 \langle \gamma \rangle} E = 0. \quad (18)$$

Depending on the amplitude of the laser field at the back of the pulse, it is possible for  $\langle P_z^l \rangle$  to increase so that

$|\langle P_z^l \rangle| \geq 1$ . Below we can see that this really takes place. Therefore, the relativistic factor at the back of the pulse can be written as

$$\langle \gamma \rangle = \{1 + |E|^2 + \langle P_z^l \rangle^2\}^{1/2}. \quad (19)$$

The conditions (14) and (15) allow us to integrate Eqs. (4) and (5). Taking into account expression (19), we obtain

$$\langle n \rangle / \langle \gamma \rangle = C_1 / (r, \xi) / [\langle \gamma \rangle - \langle P_z^l \rangle], \quad (20)$$

$$2\langle P_z^l \rangle = (1 + |E|^2) / [C_2(r, \xi) + \langle \Phi \rangle] - [C_2(r, \xi) + \langle \Phi \rangle]. \quad (21)$$

The integration constants  $C_1(r, \xi)$  and  $C_2(r, \xi)$  are determined by the values of the corresponding quantities at the end of the front of the pulse. These quantities are denoted by the subscript 0. According to Eqs. (6), (14), and (15), the variation of  $\langle \Phi \rangle$  at the back of the pulse is of the order of  $(\omega_p \tau_r)^2 \ll 1$ . Therefore, keeping this accuracy under the condition  $\langle P_z^l \rangle_0 \ll \langle \gamma \rangle_0$ , for the integration constants we obtain  $C_1(r, \xi) = \langle n \rangle_0$  and  $C_2(r, \xi) = \langle \gamma \rangle_0 + \langle P_r^l \rangle_0$ . Consequently, the solutions (20) and (21) can be written as

$$\langle n \rangle = \langle \gamma \rangle \langle n \rangle_0 / \langle \gamma \rangle_0, \quad (22)$$

$$\langle P_z^l \rangle = (|E|^2 - |E_0|^2) / 2(1 + |E_0|^2)^{1/2} + \langle P_z^l \rangle_0. \quad (23)$$

The fact that  $\langle n \rangle / \langle \gamma \rangle$  does not depend on  $\tau$  explicitly makes it possible to find the following analytical solution to Eq. (18):

$$E = E_1(\xi, r, \tau) \exp(i\omega_0 \tau), \quad (24)$$

where

$$\begin{aligned} E_1(\xi, r, \tau) &= E_1(\xi=0, r, \tau=\tau_0) J_0[2F(\xi)^{1/2}(\tau-\tau_0)^{1/2}] \\ &\quad - \int_{\tau_0}^{\tau} d\tau' J_0[2F(\xi)^{1/2}\tau'^{-1/2}] \\ &\quad \times \partial E_1(\xi=0, r, \tau-\tau') / \partial \tau' \\ &\quad + \int_0^{\xi} d\xi' J_0\{2[F(\xi)-F(\xi')]^{1/2}(\tau-\tau_0)^{1/2}\} \\ &\quad \times \partial E_1(\xi', r, \tau=\tau_0) / \partial \xi', \end{aligned} \quad (25)$$

$$F(\xi) = (\omega_p^2 / 2c) \int_0^{\xi} d\xi' \langle n(\xi') \rangle_0 / \langle \gamma(\xi') \rangle_0, \quad (26)$$

and  $J_0$  is the zeroth-order Bessel function. From Eq. (23) it follows that  $|\langle P_z^l \rangle|$  really increases at the back of the pulse, reaching the maximum value at the end of it:

$$|\langle P_z^l \rangle|_{\max} = |E_0|^2 / 2(1 + |E_0|^2)^{1/2}. \quad (27)$$

Let us return to Eq. (17). Under the conditions implied by Eqs. (14) and (15) the equation  $\text{rot} \langle \vec{P}^l \rangle|_{\varphi} = 0$  has the solution  $\langle P_r^l \rangle \approx -(c\tau_r / l_{\perp \tau}) \langle \vec{P}_z^l \rangle + \langle P_r^l \rangle_0$ , where  $\langle \vec{P}_z^l \rangle$  is the mean value of  $\langle P_z^l \rangle$  over the time interval  $\tau_r$ . Therefore, relation (17) leads to  $(c\tau_r / 2l_{\perp \tau}) |E_0| \leq \langle P_r^l \rangle_0$ . This condition can be easily met. At the same time, Eq. (17) has a transparent

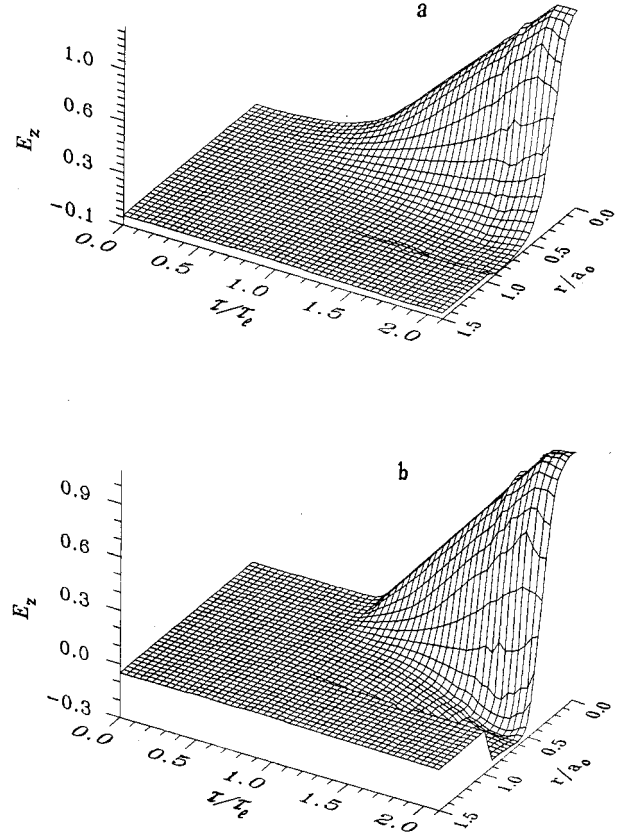


FIG. 6. Axial electrostatic field generated inside the pulse after the pulse has traveled (a) the distance  $0.5L_R$  and (b) the distance  $8L_R$ . The field is mainly concentrated in the channel and goes to zero as  $r \rightarrow \infty$ .

physical meaning:  $\langle P_r^l \rangle$  is related to radial redistribution of electrons when forming the ion channel. The fact that actually  $\langle P_r^l \rangle$  does not change significantly at the back of the pulse means that the ion channel formed by the leading front almost retains its radial structure over the time interval  $\tau_r$ .

The numerical calculations were carried out for the following values of laser pulse and plasma parameters:

$$\begin{aligned} (a_0 / \lambda_0)^2 &= 4 \times 10^2, & (\omega_p / \omega_0)^2 &= 10^{-3}, \\ (\tau_l / \tau_r)^2 &= 10^3, & |E_0|^2 &= 2.44. \end{aligned}$$

In our model the values of corresponding quantities at the end of the front determine the initial conditions for the equations for the back of the pulse. The space-time variables were normalized to the following units:  $\xi \rightarrow \xi / 4L_R$ ,  $r \rightarrow r / a_0$ , and  $\tau \rightarrow \tau / \tau_l$ , where  $L_R = \pi(a_0 / \lambda_0)^2 \lambda_0$  is the Rayleigh length. The figures presented make it possible to follow the processes of self-focusing and self-channeling of the laser pulse. The significant expulsion of electrons out of the axial region is clearly seen even at a distance of  $0.4L_R$  (Fig. 2). This process of electron ejection is accompanied by the formation of an ion channel and at a distance of  $0.5L_R$  it is virtually completed, as shown in Figs. 3–5. With the propagation of the laser pulse, the length and the width of the ion channel are increased. Even at a distance of  $L_R$ , the length of the channel exceeds half of the initial length of the laser pulse

and the width is approximately one-third of its initial width in the vacuum. The front of the pulse becomes “squashed” and its length is shortened almost two times compared to the initial length. The modulation of the envelope of the front also takes place (Fig. 4). The modulation is connected with the self-focusing and erosion of the laser beam. The erosion takes place because of diffraction. The low-power leading portion of the front diffracts almost as if in vacuum. Even at a distance of  $8L_R$  (Fig. 5) the length of the laser pulse becomes nearly equal to the length of the ion channel. One can see that at this distance the self-channeled regime of propagation is maintained without appreciable changes in the width of the ion channel and the pulse. Along with distance, the back of the pulse is also shortened. But due to the sharp cutoff of the trailing edge, its shortening is less noticeable, so the width of the ion channel at the trailing edge of the pulse remains almost unchanged. Thus the electrons ejected by the front to the periphery of the ion channel do not redistribute appreciably in the radial direction over the time  $\tau_\tau$ . According to Fig. 6, the longitudinal electric field  $E_z$  is generated at the front of the pulse and monotonically increases towards the end of the trailing edge. This field is measured in dimensionless units  $E_z = (e/mc\omega_0)(\omega_p/\omega_0)^2 E_A/\omega_0\tau_l$ . The radial width of the longitudinal field increases to the back of the pulse; at a distance of  $a_0/2$  it changes its polarity and at  $r \rightarrow \infty$  tends to zero.

For qualitative estimation we take the following characteristic values of the parameters:  $\lambda_0 \approx 1.06 \mu\text{m}$ ,  $\tau_l \approx 0.2$

$\times 10^{-12}$  s, and  $\omega_p^2 \approx 3 \times 10^{27} \text{ s}^{-2}$ . Figure 5 shows that the laser pulse travels a distance at least equal to  $8L_R$  without filamentation and significant distortion. For the above parameters, according to Fig. 6(b), we obtain  $E_A \approx 10 \text{ GV/cm}$  for the accelerating field on the axis. Any electron with the accelerating phase in such a field will gain the energy  $8L_R e E_A \approx 10 \text{ GeV}$  over a distance of  $8L_R \approx 1 \text{ cm}$ .

In conclusion, we have shown that improved conditions for the electron acceleration can be created by the interaction of an asymmetric laser pulse with plasmas. In contrast to the plasma beat-wave accelerator [6], the formation of an accelerating region by an asymmetric laser pulse is less sensitive to the nonuniformity of the plasma density profile. On the contrary, the nonuniformity may be used to change the group velocity of the laser pulse in order to keep the accelerated particles in the maximum accelerating field region for a longer time. Moreover, as shown by the numerical simulation, the accelerating field as well as the ion channel formed by the laser pulse can be sustained behind the pulse over the short fall length where the pulse intensity is terminated. Thus the proposed asymmetric laser pulse seems to be more efficient in creating favorable conditions for radial focusing and accelerating of trailing bunches of electrons in plasmas compared to the known laser wake-field accelerator schemes.

We express our gratitude to E. Khirseli and M. Tagviashvili for their assistance in the work. This work was supported by the International Science Foundation, Grant No. RV M000.

- 
- [1] P. Sprangle *et al.*, Phys. Rev. Lett. **69**, 2200 (1992); N. A. Andreev *et al.*, Pisma Zh. Éksp. Teor. Fiz. **55**, 551 (1992) [JETP Lett. **35**, 571 (1992)]; J. Krall *et al.*, Phys. Rev. E **48**, 2157 (1993); E. Esarey *et al.*, Phys. Fluids B **5**, 2660 (1993); V. I. Berezhiani and I. G. Murusidze, Phys. Lett. A **148**, 338 (1990); L. A. Abramian *et al.*, Zh. Éksp. Teor. Fiz. **75**, 952 (1992) [Sov. Phys. JETP **75**, 978 (1992)]; S. V. Bulanov, F. Pegoraro, and A. M. Pukhov, Phys. Rev. Lett. **74**, 710 (1995); P. K. Kaw, A. Sen, and T. Katsouleas, *ibid.* **68**, 3172 (1992).
- [2] D. P. Garuchava, Z. I. Roštomashvili, and N. L. Tsintsadze, Fiz. Plazm. **12**, 1341 (1986) [Sov. J. Plasma Phys. **12**, 776 (1986)]; D. P. Garuchava, N. L. Tsintsadze, and D. D. Tskhakaya, in *Proceedings of the Tenth European School on Plasma Physics, Tbilisi*, 1990, edited by N. Tsintsadze (World Scientific, Singapore, 1990), p. 465.
- [3] N. L. Tsintsadze, Phys. Scr. **41**, 267 (1990); P. C. Barnes, T. Kurki-Suonio, and T. Tajima, IEEE Trans. Plasma Sci. **PS-15**, 154 (1987); P. Sprangle, C. M. Tang, and E. Esarey, *ibid.* **PS-15**, 145 (1987); G. Z. Sun *et al.*, Phys. Fluids **30**, 526 (1987); W. B. Mori *et al.*, Phys. Rev. Lett. **60**, 1295 (1988); A. B. Borisov *et al.*, Phys. Rev. A **45**, 5830 (1992).
- [4] D. P. Garuchava and M. N. Tagviashvili, in *Proceedings of the International Conference on Plasma Physics, Foz do Iguaçu-pr-Brazil, 1994*, edited by P. H. Sakanaka, E. del Bosco, and M. V. Alves (Sao Jose dos Campos, 1994), Vol. 1, p. 233.
- [5] J. Krall *et al.*, Phys. Plasmas **1**, 1738 (1994); E. Esarey *et al.*, Phys. Fluids B **5**, 2690 (1993).
- [6] T. Tajima and I. M. Dawson, Phys. Rev. Lett. **43**, 263 (1979); C. E. Glayton *et al.*, *ibid.* **70**, 37 (1993); F. Amiranoff *et al.*, *ibid.* **74**, 5220 (1995).